Transients of the photoluminescence intensities of the electron-hole droplets in pure and doped Ge

M. Chen, S. A. Lyon, D. L. Smith, and T. C. McGill
California Institute of Technology, Pasadena, California 91125
(Received 9 November 1977)

We have measured the electron-hole-droplet (EHD) luminescence intensities in pure and doped Ge as a function of time at 2 and 4.2°K. Surface-excitation pulses 50 to 100 μsec in length were used. The EHD intensities were found to reach steady-state levels after several tens of microseconds. The decay of the EHD luminescence intensity in pure Ge at 4.2°K was too slow to be explained by the previously accepted model. The decay at 2°K of the luminescence intensity of the EHD in Ge doped with $\sim 10^{15}$ cm^{-3} of impurities was found to be identical to that in pure Ge, i.e., exponential decay with lifetime of 37 μsec; however, very little effect due to evaporation of excitons was observed at 4.2°K. A new model of the decay of the luminescence intensity of EHD is presented. This model is based on the existence of a cloud of EHD's and it incorporates (i) exciton flow among EHD's in the cloud and (ii) exciton diffusion out of the cloud. This model explains the decay of the EHD luminescence in both pure and doped Ge. In particular, this model shows that the size of the cloud of EHD's can affect the EHD decay at high temperatures and the reduction of free-exciton diffusion length can shut off the effect of exciton evaporation on the decay transients in doped Ge.

I. INTRODUCTION

The existence of a metallic liquid phase of electron-hole pairs in Ge at cryogenic temperatures is by now well established.[1] A wide variety of experiments, mostly using optical excitation on high-purity Ge, have been used to determine many properties of this electron-hole liquid. Light scattering[2,3] and junction noise[4] experiments have demonstrated that the electron-hole liquid is produced in the form of a cloud of electron-hole-droplets (EHD) in Ge. The size of the EHD can be as big as 10 μm.[5] The kinetics of formation and decay of these EHD's have been the subject of numerous investigations. The decay of the EHD has been carefully studied using cyclotron resonance,[6] luminescence intensity decay,[7-9] and far-infrared absorption.[10] More recently, the growth of the EHD has been examined using both surface excitation[11] and volume excitation.[12]

In the volume-excitation experiment,[12] EHD's were observed to nucleate from a supersaturated free-exciton (FE) gas. The rate of growth of droplet intensity agreed with nucleation-theory predictions.[13,14] Inhomogeneous excitation and carrier transport away from the excited surface complicate the situation in the surface-excitation experiments. Pokrovskii[15] and Hensel *et al.*,[6] have proposed a model for the decay of the EHD which may be applied to the surface-excitation experiments. This model is based on the average rate equations for the EHD

$$\frac{d\nu}{dt} = -\frac{\nu}{\tau} - aT^2 e^{-\phi/kT}\nu^{2/3} + b\nu^{2/3}\bar{n}_{ex}\,, \tag{1}$$

and for the FE

$$\frac{d\bar{n}_{ex}}{dt} = -\frac{\bar{n}_{ex}}{\tau_{ex}} + (aT^2 e^{-\phi/kT}\nu^{2/3} - b\nu^{2/3}\bar{n}_{ex})N\,. \tag{2}$$

In (1) and (2), ν is the average number of electron-hole pairs in an EHD, τ and τ_{ex} are, respectively, the EHD and FE total lifetime, a is the Richardson-Dushman constant,[16] ϕ is the work function of the EHD, T is the temperature, $\bar{n}_{ex}$ is the FE density, and N is the number density of droplets. The constant b is equal to $v_{th}\pi(3/4\pi n_0)^{2/3}$ where v_{th} is the average thermal velocity of the exciton and n_0 is the pair density of an EHD. The three terms on the right-hand side of Eq. (1) are, respectively, from left to right, bulk recombination, evaporation, and FE backflow rates. Usually $\bar{n}_{ex}$ is assumed to be zero during the decay so that EHD's are decoupled from the FE and from each other. With the assumption of $\bar{n}_{ex}$ equal to zero, Eq. (1) can be readily solved to yield

$$\nu(t) = \nu(0)\{[e^{(t_c-t)/3\tau} - 1]/[e^{t_c/3\tau} - 1]\}^3\,, \tag{3}$$

with

$$t_c = 3\tau \ln[1 + \nu(0)^{1/3}/a\tau T^2 e^{-\phi/kT}]\,. \tag{4}$$

At low temperatures the evaporation rate is small compared to the recombination rate and the EHD decay is nearly exponential with a time constant equal to τ. At higher temperatures evaporation becomes important, and hence, the EHD decay is faster than the exponential decay expected at low temperatures. By adjusting t_c in Eq. (3), one can fit the experimentally observed EHD decay transients quite well. However, if high excitation power is used,[8,9] the value of t_c needed to fit the data

leads to values for $\nu(0)$ or initial droplet radii which are too large compared with the results of light scattering experiments.[2,3]

Recently, Ashkinadze and Fishman[9] have suggested that one can explain the decay at 4.2 °K by assuming that the FE density is independent of time, the diffusion of FE may be neglected, and the capture of FE dominates the decay. This model neglects the spatial variation of FE and EHD densities.

In the case of doped Ge, very limited EHD luminescence decay data exist in the literature[17] and these data have not been used to extract any other information about the EHD and FE.

In this paper we present data on the growth and decay of the EHD and FE luminescence intensity in pure and doped Ge which are excited with long GaAs laser pulses (50–100 μsec). We found that it takes several tens of microseconds for the EHD luminescence intensity to reach a steady state after the excitation is abruptly turned on (rise time <1 μsec). The rise of the EHD intensity in our experiments cannot be adequately described by the nucleation theory due to the inhomogeneity of excitation. Our results of the decay of the EHD signal for pure Ge and Ge doped with 10^{15} cm^{-3} of impurities show that the widely accepted single-drop model of decay is inadequate in many experimental situations. A new model based upon the existence of a cloud of EHD's and the diffusion equation for FE's is presented. The diffusion equation approach can deal with the evaporation and backflow of FE across the surface of a droplet in a consistent manner. This model quantitatively explains the decay transients of EHD in both pure and doped Ge. In particular, it is found that a reduction of the FE diffusion coefficient in the ~10^{15} cm^{-3}-doped Ge can lead to the observed curtailment of the net FE evaporation by droplets.

This paper is organized as follows. In Sec. II, we outline the details of sample preparation and experimental procedure. Section III is divided into three parts containing, respectively, the experimental results for pure lightly doped (impurity concentration $N_i \sim 10^{15}$ cm^{-3}), and heavily doped ($N_i \sim 10^{16}$ cm^3) Ge samples. In Sec. IV, the model for the EHD and FE decay is presented. Discussion of experimental results and comparison of experiment with theory are presented in Sec. V. The summary is in Sec. VI.

II. EXPERIMENT

Samples were prepared from Ge slices which have areas between 80–500 mm^2 and with one exception thickness of at least 2 mm. One of the high purity samples used was 1 mm thick. The results from this 1-mm sample were compared to those from a 2-mm-thick high-purity sample to determine the effect of sample thickness. The flat faces of the samples were first mechanochemically polished to produce smooth surfaces. They were then lightly etched in a 5:1 HNO_3:HF solution to minimize the surface damage created by the polishing step. Prior to mounting them for any experiment, they were rinsed with methanol and dried.

Photoexcitation was provided by a RCA SG2007 GaAs laser diode. Both the laser and the sample were mechanically attached to a copper sample block with the laser sitting a few mm perpendicularly above the sample's flat face. The GaAs laser was driven by current pulses of 50 or 100 μsec duration. A fixed duty cycle of 2% was used. Current was varied between 200 and 600 mA producing peak powers (as determined using a calibrated Si photodiode and uncorrected for reflection losses at the sample surface) between 0.06 and 0.22 W. The laser light spot on the sample as determined with an infrared image converter was about 1 mm in diameter. A vacuum-regulated liquid-He bath was used to achieve the required temperatures. Temperature was monitored with a calibrated Ge sensor mounted in the sample block close to the sample.

The radiation emitted from the excited face of the sample was collected and focused onto the entrance slit of a Spex 1400-II spectrometer by two lenses. The lens combination had a magnification factor of about 3. The spectrometer was set to 708.6 meV, and the slits were opened to a width of 3 mm. This arrangement allowed radiation within a 30-Å (1.2-meV) band, centered on the peak of the LA-phonon assisted EHD emission line to pass through the spectrometer. An elliptical mirror mounted at the exit slit of the spectrometer focused the output from the spectrometer onto an InAs photovoltaic detector operated at 195 °K. The detector output was fed through a current amplifier to a boxcar integrator and recorded on a strip-chart recorder. A boxcar gate width of 2 μsec was used in all experiments.

The shape of the excitation light pulse reported was determined by placing the detector directly in front of the Dewar window and measuring the scattered laser light. By using this technique, any shift of the GaAs laser frequency during the laser pulse would not affect the measured results. Since the rise time of the laser pulse is much faster than that of our detection system, the measured rise time of the laser pulse yielded directly our system response time. This response time was less than 5 μsec. The actual rise time of the light pulse is limited by the rise time of our cur-

rent pulser and is less than 20 nsec. The dependence of our detection system's rise time on the intensity of light falling on the detector was checked. This rise time was found to be constant for the range of light levels investigated in our experiments.

III. EXPERIMENTAL RESULTS

A. Pure germanium

In Figs. 1 and 2, respectively, we show the EHD luminescence intensity versus time at 2 and 4.2 °K. The sample is a 2 mm thick high-purity Ge crystal. At 2 °K the transients for pump powers of 0.06 and 0.09 W were identical. The rise of the EHD intensity was nonexponential and the 0%–90% rise time was about 46 μsec. The decay was exponential with a lifetime of 37 μsec. This decay time is in good agreement with previous published results.[6-8] The 0%–90% rise time of the EHD signal at 4.2 °K was about 40 μsec. The decays at 4.2 °K were nonexponential and showed finite cutoff times which increased with increased pump power. The output of our GaAs laser, shown by the dash-dot curves, drooped during the current pulse as a result of the temperature rise of the laser. Because of this droop, the rise time of the EHD signal that we measured was somewhat smaller than the step-response time of the EHD luminescence.

The qualitative behavior of the decay of EHD luminescence under our excitation conditions is similar to that observed using short intense GaAs laser pulses.[6-8] The 4.2 °K decay transients we observed can be fitted very well by Eq. (3) using the observed EHD lifetime at 2 °K and suitable t_c's. However, the required t_c's were between 45 and 60 μsec. These large t_c's yield, using Eq. (4) and the values for the parameters given in Ref. 5, initial

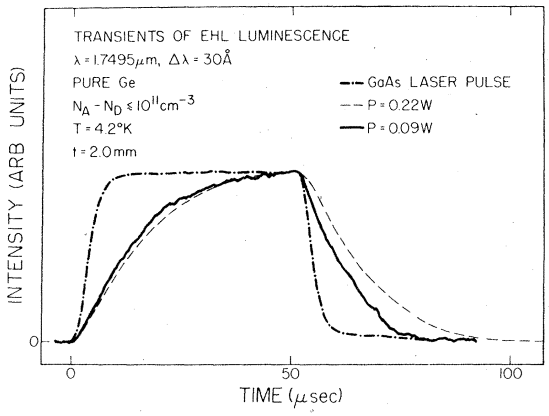

FIG. 1. Transients of the photoluminescence intensity of the electron-hole liquid in pure Ge at 4.2 °K. The thickness of the sample is denoted by t.

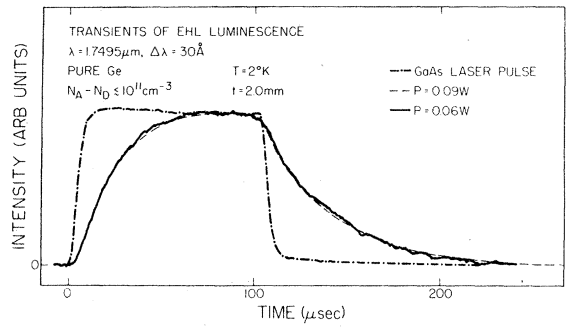

FIG. 2. Transients of the photoluminescence intensity of the electron-hole liquid. All parameters are the same as those of Fig. 1 except the temperature is 2 °K. Note the difference in the horizontal scales of this figure and Fig. 1.

radius of the EHD of about 0.3 mm. In unstressed Ge, droplet radii of this order are in disagreement with the results of light scattering experiments which show for a wide range of excitation conditions that the droplet radius does not exceed about 10 μm.[2]

The sensitivity of the transients to sample thickness was checked by repeating the measurements for a 1 mm thick sample. In this 1-mm sample the growth and decay of the EHD signal were faster at both 4.2 and 2 °K. We have also performed these experiments on the 2-mm sample after we have damaged that sample's back surface by sandblasting. The transients of the EHD luminescence for this 2-mm sample were found to be unchanged by the damage to the back surface. Thus, we establish that the EHD cloud generated in the samples in our experiments extends between 1 and 2 mm away from the excited surface of the sample.

In Fig. 3 a transient of the FE luminescence signal along with the concurrent, normalized EHD signal from the 2 mm thick pure Ge sample is shown. We interpret the FE signal to be composed

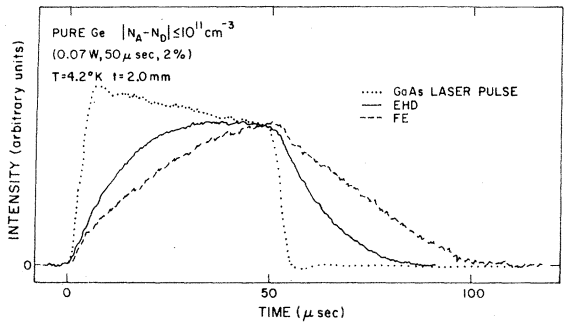

FIG. 3. Transients of the photoluminescence intensity of the electron-hole liquid and the concomitant free exciton. The intensities are normalized to the same height at the end of the laser pulse. The ringing on the laser pulse is an artifact caused by the amplifier for the detector.

of the sum of two components. The first one is due to FE's created directly by the laser. This component has approximately a 7 μsec (FE lifetime)[8] rise and fall time at the beginning and the end of the laser pulse, and it is constant during the middle of the pulse. The second component is attributed to the increase of the volume occupied by FE's as the cloud of EHD's expands to its steady-steady size. The growth and decay transients of the FE and EHD signal we observed are qualitatively different from the results of the volume-excitation experiment.[12] In particular, we detected no reduction in the FE intensity which should be associated with the nucleation and growth of EHD's.[12] We attribute these differences to the inhomogeneities of the excitation in our experiments. The decay of the FE signal is approximately linear with time and the EHD's decay in the presence of a non-negligible concentration of FE's.

B. Lightly doped germanium ($N_i \sim 10^{15}$ cm^{-3})

The EHD luminescence transients from a Ge sample with 4×10^{15} As/cm^3 at 4.2 and 2 °K are shown in Fig. 4(a) and 4(b), respectively. The transients at 2 °K for $P = 0.09$ and 0.06 W were essentially identical. At 2 °K the 0%–90% rise time was ~65–70 μsec while the decay was exponential with a lifetime of 37 μsec. This lifetime is identical to the lifetime of EHD in pure Ge. However, unlike pure Ge, the transients, in particular the decays, were not very sensitive to temperature between 2 and 4.2 °K. In addition, the transients at both 2 and 4.2 °K were only slightly pump-power dependent. Essentially identical results were observed for a 2×10^{15} Ga/cm^3 sample. Thus, for temperature at least as high as 4.2 °K, the EHD

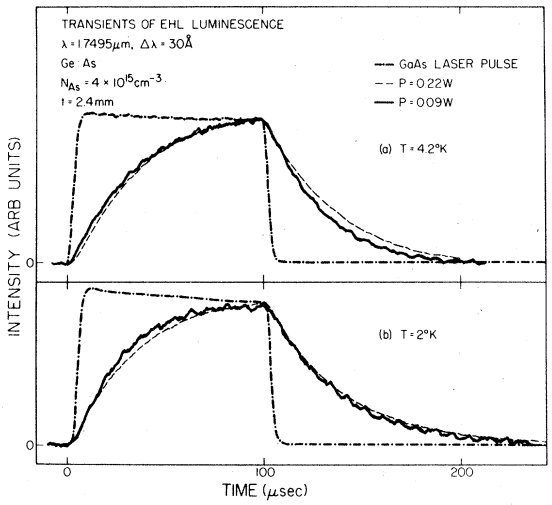

FIG. 4. Transients of the photoluminescence intensity of the electron-hole liquid doped Ge.

luminescence intensity decay in lighly doped Ge is determined principally by the EHD lifetime, i.e., FE evaporation from EHD's does not play a large role in the decay of EHD.

The work function of the EHD in Ge with $N_i \sim 10^{15}$ cm^{-3} has been found, experimentally and theoretically,[18] to be identical to that in pure Ge. We have shown above that the EHD lifetime was also unaffected by doping of this level. Thus, the recombination and evaporation terms in Eq. (1) cannot be affected by doping level of ~10^{15}cm^{-3}. The reduction of the net evaporation rate for EHD in doped Ge must come about by an increase in the backflow rate caused by impurities. In the theory section of this paper, we shall show that a reduction of FE diffusion coefficient, caused by impurity atoms, could lead to increased backflow rate in doped Ge.

C. Heavily doped germanium ($N_i \sim 10^{16}$ cm^{-3})

The photoluminescence spectra of heavily doped Ge are complicated by impurity induced emissions.[19] Only the phonon-assisted lines in Ge:As

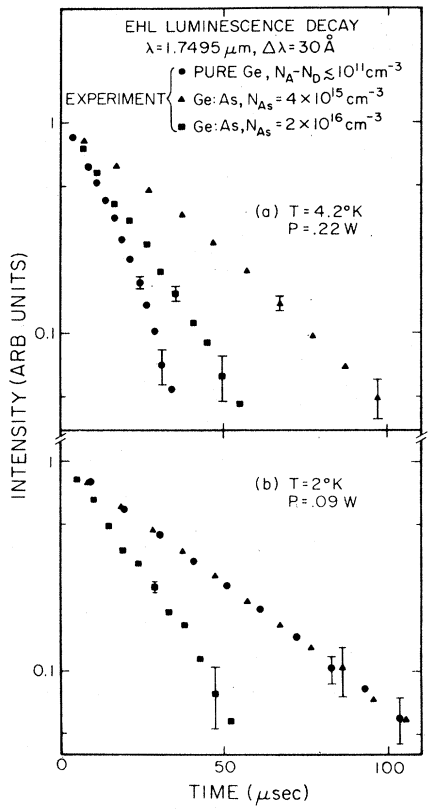

FIG. 5. Normalized luminescence intensity of the electron-hole droplets in heavily doped Ge on semilog plot. The decay transients of the electron-hole-droplet luminescence of pure and lightly doped Ge are also shown for comparison.

(and perhaps Ge:P) for $T \leq 4.2$ °K may be interpreted to reflect the properties of the EHD in doped Ge. We report here the results for a Ge crystal with 2×10^{16} As/cm^3. The 0%-90% rise time at 4.2 °K was 50 μsec for 0.22-W pumping and about 35 μsec for 0.09-W pumping power. At 2 °K the risetime was 50 μsec for both 0.22- and 0.09-W excitation power. The decay transients are shown on a semilog plot in Fig. 5 where we have also shown the decay curves for pure and lightly doped Ge for a comparison. We observed that the decay of the EHD at 2 °K in heavily doped Ge:As was exponential with a time constant of about 23 μsec. This EHD lifetime is considerably shorter than the 37 μsec EHD lifetime in pure Ge. As in lightly doped Ge, the decays in heavily doped Ge showed very little effect of evaporation at both 2 and 4.2 °K.

IV. MODEL FOR DECAY

A. Description of physics

The EHD distribution in the sample at the end of the excitation pulse is complex. The EHD cloud is spatially nonuniform and not simple in shape.[2] In addition, droplets may be in motion.[20] Nonetheless, we can gain an understanding of the decay of the EHD and FE using a somewhat idealized model which retains the essential physics.

In this model, the EHD cloud is assumed to be spherical in shape and situated in an infinite Ge crystal. Inside this sphere of radius R_c the density of EHD's is taken to be spatially uniform while outside this sphere the EHD density is taken to be zero. The exciton density inside the cloud is nonuniform due to the presence of EHD's. This spatially varying exciton density has an average value of $\bar{n}_{ex}$. Outside the cloud, the exciton density is determined by exciton diffusion from the edge of the cloud. A schematic illustration of this model is shown in Fig. 6. Exciton concentrations in and out of the cloud are obtained through solutions to the exciton diffusion equation. This diffusion equation approach allows us to (i) treat the *net evaporation* rate, i.e., the sum of evaporation and backflow rates in Eq. (1), in a reasonable way, and (ii) incorporate flow of excitons outside of the cloud and the resulting shrinking of the cloud with time. Both of these aspects were not considered in the single-drop model.

There are three decay paths for electron-hole pairs: recombination inside an EHD, recombination of FE in the cloud, and recombination of FE after diffusing away from the edge of the cloud. To determine the rates for these three paths, two main problems have to be solved. First is the diffusion of excitons away from the cloud, causing

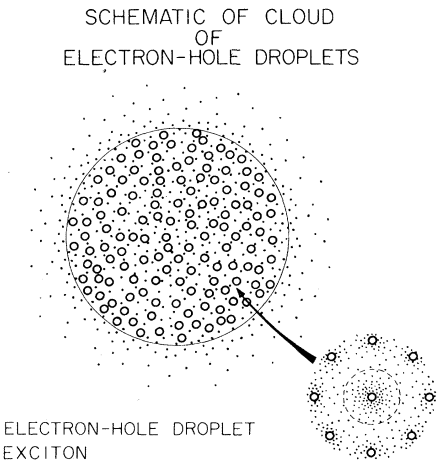

FIG. 6. Schematic illustration of the cloud of electron-hole droplets and free-excitons. The radius of the cloud is R_c. Inset shows an enlarged view of an electron-hole droplet surrounded by neighboring electron-hole droplets. The central electron-hole droplet needs to supply excitons only into the volume bounded by R_s (dashed line).

the cloud to shrink. For this we solve the exciton diffusion equation outside the cloud with the boundary conditions that the exciton density be equal to zero at infinity and equal to $\bar{n}_{ex}$ at the cloud edge. The second problem is the calculation of $\bar{n}_{ex}$. The inset in Fig. 6 depicts the situation in the body of the cloud and is the basis for the calculation of the average exciton density. The close proximity of the droplets, interdrop distances being much less than an exciton diffusion length for pure material, implies that each drop on the average only supplies excitons to its immediate vicinity. Each droplet is assigned a spherical volume of radius R_s as shown in the figure by the dashed line, and the condition is imposed that the net flux of excitons out of this volume vanishes. This boundary condition should be contrasted with that in a single-drop picture in which the excitons can diffuse out to infinity. Solving the diffusion equation within the region bounded by R_s and averaging the exciton density over the volume of this region gives the average exciton density within the cloud. Each droplet in the body of the cloud shrinks as it must supply both the pair recombination current within itself and the exciton recombination current in the volume bounded by R_s. Thus, the number of pairs bound in droplets and the associated luminescence signal decrease both through the shrinking of individual droplets and the shrinking of the cloud as a whole.

B. Mathematical description

The differential equation for the decay of the cloud is determined by equating the rate of change

of the total number of pairs in the cloud to the sum of the recombination rate for pairs bound in droplets, the recombination rate for excitons within the cloud, and the diffusion current of excitons away from the cloud at its surface:

$$\frac{d}{dt}(V_c N_0 + V_c \bar{n}_{ex}) = \frac{-V_c N_0}{\tau} - \frac{V_c \bar{n}_{ex}}{\tau_{ex}} - J_D\big|_{R_c}, \qquad (5)$$

where V_c is the volume of the cloud, N_0 the density of pairs bound in EHD's [(EHD density)$\times$(fill factor)], and J_D the diffusion current of free excitons, here evaluated at the radius of the cloud R_c. Distributing the time derivative, we obtain two terms one describing the change in V_c and the other change in total density of pairs. If we assume that recombination only affects the density of pairs in the cloud without changing its size while exciton diffusion causes the cloud to shrink but only perturbs the pair density slightly near the surface, then Eq. (5) separates giving

$$(N_0 + \bar{n}_{ex})\frac{dR_c}{dt} = |D\nabla n_{ex}|_{R_c}, \qquad (6)$$

and

$$\frac{d}{dt}(N_0 + \bar{n}_{ex}) = -\left(\frac{N_0}{\tau} + \frac{\bar{n}_{ex}}{\tau_{ex}}\right), \qquad (7)$$

where D is the exciton diffusivity, and thus $-D\nabla n_{ex}|_{R_c}$ is the exciton flux evaluated at the surface of the cloud.

To obtain the exciton diffusion current on the right-hand side of Eq. (6), we need to solve the diffusion equation governing the FE's outside the EHD cloud,

$$\frac{\partial n_{ex}}{\partial t} = D\nabla^2 n_{ex} - n_{ex}/\tau_{ex}, \qquad (8)$$

where n_{ex} is a function of both t and the distance r from the center of the cloud. The boundary conditions to be satisfied are

$$n_{ex} = \bar{n}_{ex} \quad \text{at} \quad r = R_c(t), \qquad (9)$$

and

$$n_{ex} = 0 \quad \text{at} \quad r = \infty. \qquad (10)$$

Equation (8) is coupled to the equation for R_c through boundary condition Eq. (9). The equation for R_c is

$$\frac{dR_c}{dt} = \frac{|D\nabla n_{ex}|_{R_c}}{\bar{n}_{ex} + n_0 F}. \qquad (11)$$

In Eq. (11) the fill factor F is defined to be the fractional volume of the cloud containing electron-hole liquid. These equations can be solved for (dR_c/dt) in terms of $R_c(t)$ and $\bar{n}_{ex}(t)$.

To determine the decay of EHD and FE inside the cloud Eq. (7), it is necessary to solve the exciton diffusion Eq. (8) for the region surrounding a given droplet with two boundary conditions: First, at the surface of the drop, $r = R_D(t)$, diffusion current away from the droplet equals evaporation rate minus backflow rate, or

$$-4\pi R_D^2 D \left.\frac{\partial n_{ex}}{\partial r}\right|_{R_D} = aT^2 e^{-\phi/kT}\nu^{2/3} - 4\pi R_D^2 n_{ex} v_{th}. \qquad (12)$$

Second, no exciton diffusion current flows across R_s, that is,

$$\nabla n_{ex} = 0 \quad \text{at} \quad r = R_s(t). \qquad (13)$$

Neglecting the finite FE and EHD lifetimes, the FE evaporation rate can be estimated from the equilibrium density of FE (n_{ex}^0) by detailed balance,

$$aT^2 e^{-\phi/kT}\nu^{2/3} = 4\pi R_D^2 n_{ex}^0 v_{th}. \qquad (14)$$

The excitons in the cloud are coupled to the droplets through the equation

$$\frac{d\nu}{dt} = -\frac{\nu}{\tau} - J_D\big|_{R_D}, \qquad (15)$$

where $J_D|_{R_D}$ is the exciton diffusion current evaluated for a drop radius of R_D,

$$\frac{dR_D}{dt} = -\frac{R_D}{3\tau} - \frac{|D\nabla n_{ex}|_{R_D}}{n_0}. \qquad (16)$$

The exciton diffusion equation can be solved and substituted into Eq. (16) to yield dR_D/dt as a function of time.

From the two parts of the problem Eq. (6) and (7), two equations are obtained

$$\frac{dR_D}{dt} = f(R_D) \qquad (17)$$

and

$$\frac{dR_c}{dt} = g(R_D, R_c). \qquad (18)$$

The functions f and g are given in the Appendix. A straightforward numerical integration of f and g yields $R_D(t)$ and $R_c(t)$. From $R_D(t)$ and $R_c(t)$ we obtain

$$I_{EHD} \sim R_c(t)^3 F(t) \qquad (19)$$

and

$$I_{FE}(t) \sim \tfrac{4}{3}\pi R_c^3 \bar{n}_{ex}(t) + M_{ex}(t)\,, \qquad (20a)$$

where M_{ex} is the number of excitons outside the cloud. To determine M_{ex} we numerically integrate the source-sink equation with respect to time

$$M_{ex} = \int_0^t \left(4\pi R_c^2 |D\nabla n_{ex}|_{R_c} - \frac{M_{ex}}{\tau_{ex}}\right) dt' + M_{ex}(0)\,, \qquad (20b)$$

where $M_{ex}(0)$, the number of excitons outside the cloud at $t = 0$, is calculated from the initial conditions.

During and at the end of the laser pulse, a generation term must be added to the left-hand side of Eq. (12). This generation term drives the exciton gradient at each droplet surface positive so that excitons can flow into droplets during the time the laser is on. It is obvious that since we have not introduced the generation term, we cannot start out with the correct initial condition. In fact, our solution assumes an initial condition such that the exciton gradient is negative at the surface of each droplet. However, since FE decay is fast, we expect the exciton density to relax from that at the end of the laser pulse to the one we assume in about one exciton lifetime. This relaxation can be observed in the FE transient in Fig. 3. Thus, our solution should be accurate to describe the decay transients after about one exciton lifetime from the end of the laser pulse.

V. RESULTS OF CALCULATION AND COMPARISON WITH EXPERIMENT

In this section, the calculated decay transients of the EHD and FE intensity will be presented and compared to experimental data. The theoretical curves presented in Fig. 7 were calculated for three different initial cloud radii. Values of the parameters used in the calculation are listed in Table I along with the values of the same parameters reported in the literature. Within experimental uncertainty, the values we used to generate the curves in Fig. 7 are the same as those found in the literature. Figure 7(a) shows the calculated EHD luminescence decay transient, normalized to unity at the start of the decay. The corresponding curves for the FE are shown in Figure 7(b). At 4.2 °K, an increase of $R_c(0)$ causes the decay to be longer because for larger $R_c(0)$, the initial surface to volume ratio is smaller, and this lessens the importance of exciton diffusion away from the cloud. Spatially resolved light absorption experiments at 4.2 °K show[21] that different initial $R_c(0)$ can be created by using different excitation powers. It can be seen in Fig. 7, that there are clear differences between the three FE curves making them a sensitive, independent check on the model. In particular, these results are

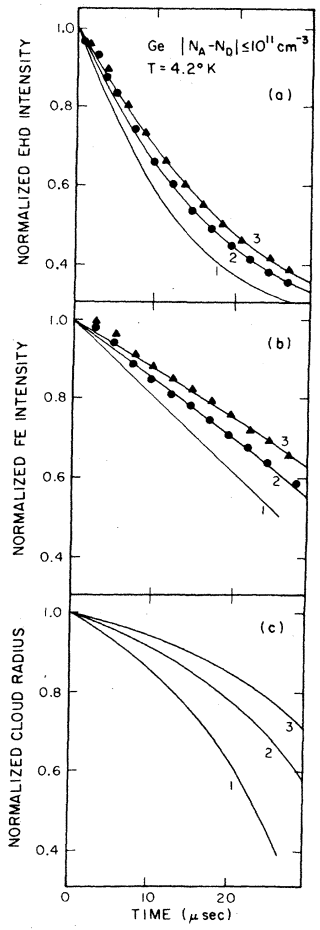

FIG. 7. Results of calculations of the model for 4.2 °K. The parameters used are appropriate for pure Ge and are given in Table I. The initial radii of the cloud for curves 1, 2, and 3 are 1.0, 1.4, and 1.8 mm, respectively. Experimental results for high-purity Ge are shown for comparison; pump powers used are (▲) 0.14 W and (●) 0.09 W.

very different from the solutions to the average equations in which there is no boundary to the region occupied by EHD's. Experimental result of the EHD and FE decay transients for two different pump powers are also shown in Fig. 7. It can be seen that excellent agreement is obtained for both the EHD and the FE curves when reasonable values for the parameters are used in the calculation. There are two points that should be noted, however. First, different parameters can offset each other, e.g., reducing the exciton diffusion length slows down the decays but this may be offset by increasing the equilibrium density of excitons which speeds up the decay. Second, light absorption experiments[21] have shown that exciton recombination current at the Ge surface is not negligibly small at 4.2 °K. Thus, our model is qualita-

TABLE I. Values of parameters used in the model.

Parameter	Values used in calculations for Fig. 7	Values found in the literature
EHD lifetime τ	37 μsec	36–45 μsec [a–c]
FE lifetime τ_{ex}	7 μsec	6–8 μsec [c,d]
Equilibrium density of FE $\bar{n}_{ex}^0$		
2 °K	7×10^{11} cm^{-3}	7×10^{11} cm^{-3} [e]
4.2 °K	3×10^{14} cm^{-3}	5×10^{14} cm^{-3} [e]
Pair density in the EHD n_0		
2 °K	2×10^{17} cm^{-3}	2.1×10^{17} cm^{-3} [e]
4.2 °K	2×10^{17} cm^{-3}	2.4×10^{17} cm^{-3} [e]
Initial EHD radius $R_D(0)$		
2 °K	2 μm	2 μm [f]
4.2 °K	10 μm	~10 μm [g]
FE diffusion length l_x	0.8 mm	~1 mm [h,i]
Fill factor F	2%	1%–2% [j,f]
Initial cloud radius $R_c(0)$	1.4–1.8 mm	1–2 mm [k,j]

[a] Reference 6.
[b] Reference 7.
[c] Reference 8.
[d] V. Marello, T. C. McGill, and J. W. Mayer, Phys. Rev. B 13, 1607 (1976).
[e] G. A. Thomas, A. Frova, J. C. Hensel, R. E. Miller, and P. A. Lee, Phys. Rev. B 13, 1692 (1976).
[f] J. M. Worlock, T. C. Damen, K. L. Shaklee, and J. P. Gordon, Phys. Rev. Lett. 33, 771 (1974).
[g] Reference 5.
[h] Reference 15.
[i] Reference 22.
[j] Reference 21.
[k] Reference 2.

tively correct in that the essential physics has been retained, but it is difficult to get accurate quantitative results from our model. Figure 7(c) shows plots of $R_c(t)$ corresponding to the cases shown in Figs. 7(a) and 7(b). At 4.2 °K, it is seen that the shrinking of the cloud of EHD's is as important as the shrinking of individual droplets in causing the decay in the droplet luminescence intensity. This collapse of the EHD cloud has been observed in temporally and spatially resolved absorption experiments.[21]

Our model also correctly describes the EHD decay at 2 °K. At this lower temperature when the importance of exciton evaporation is reduced, the EHD lifetime is the dominant factor in determining EHD luminescence intensity decay. At 2 °K, R_c does not change noticeably with time because $\bar{n}_{ex}$ is so small that FE recombination current cannot significantly affect EHD decay.

Shaklee[3] has reported transient light scattering results which show that the drop radius decays more slowly at 2 °K than expected for our model. We do not understand this disagreement at the present time.

Under the same excitation conditions, the initial cloud radius, initial fill factor, and exciton diffusion length can be different in pure Ge and Ge doped with about 10^{15} cm^{-3} of impurities. Spatial luminescence intensity scans show that the cloud of EHD's does not penetrate as deeply in lightly doped Ge as in pure Ge,[22,23] so $R_c(0)$ should be smaller in lightly doped Ge compared to pure Ge. This fact, coupled with the observation that the total luminescence intensities from pure and doped Ge do not differ significantly, implies a larger fill factor in doped Ge. Neutral impurity scattering of excitons can significantly alter the exciton diffusion length at the 10^{15} cm^{-3} doping level. Figure 8(a) shows calculations for 4.2 °K for various initial cloud radii, fill factors, and exciton diffusion lengths. For curve 1, an initial radius of 0.05 mm was assumed and the fill factor has been increased to 10% in keeping with the greater confinement of the EHD's. The exciton diffusion length is still

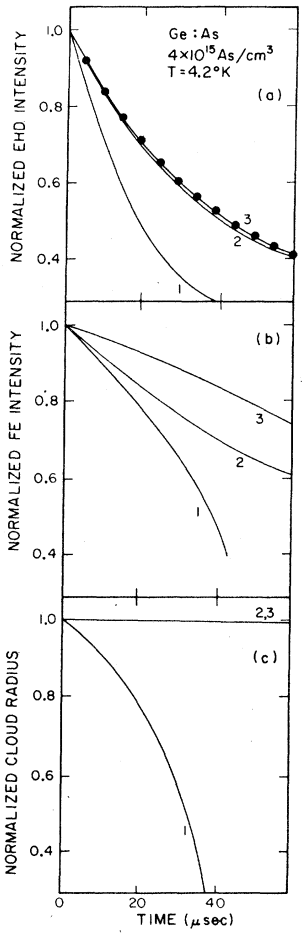

FIG. 8. Results of calculations of the model for 4.2 °K. Curve 1: FE diffusion length: 0.8 mm; fill factor: 10%. Curve 2: FE diffusion length: 0.016 mm; fill factor: 2%. Curve 3: FE diffusion length: 0.016 mm; fill factor: 10%. Initial cloud radius for all three curves is 0.5 mm; all other parameters are the same as those for pure Ge given in the text. Experimental results of the luminescence intensity decay of the EHD in a Ge sample with 4×10^{15} cm^3 are shown as the dots.

$l_x = 0.8$ mm. The decay is seen to be slower in this case compared to pure Ge [Fig. 7(a)] but is still far from being exponential. Curve 2 assumes $R_c(0) = 0.5$ mm, fill factor = 2%, and $l_x = 0.016$ mm. Comparison of curves 1 and 2 shows the much greater importance of diffusion length over fill factor in slowing down the decay. Curve 3 incorporates all the expected changes for doped Ge with $R_c(0) = 0.5$ mm, $l_x = 0.016$ mm, and a fill factor of 10%. As can be seen from Fig. 8(a), altering the parameters to those for doped Ge dramatically changes the decay curves, causing the luminescence transients to become nearly exponential for temperature as high as 4.2 °K. Excellent agreement with the experimental data, shown as dots in Fig. 8(a), is obtained. It should be noted that the value for exciton diffusion length in the doped material was determined through fitting the luminescence decays and has not been determined independently. Figure 8(b) shows the calculated decay curves for FE corresponding to the cases in Fig. 8(a). The decay time of the FE is controlled by the evaporation of excitons from droplets and is, therefore, directly related to the EHD lifetime. For the case corresponding to lightly doped Ge, curve 3, the FE decay is expected to be very slow compared to pure Ge. Figure 8(c) shows the calculated $R_c(t)$ using the same parameters as those used for the corresponding curves in Fig. 8(a) and 8(b). These curves illustrate clearly that reducing the diffusion length stops the escape of excitons from the cloud and the reduction of R_c with time. Merely increasing the fill factor as for curve 1 does not accomplish this and consequently the calculated decay is much too fast compared to experiment. We emphasize that the net evaporation of excitons from droplets must be shut off in order to account for the long decays observed for lightly doped Ge.

The reduction of free exciton diffusion length in doped Ge implies a short exciton diffusion tail and, therefore, fewer excitons around each drop. Therefore, it is expected that the relative EHD to FE intensity should be small while EHD's are decaying. This reduction of FE intensity for Ge is observed experimentally. Our model predicts, as observed experimentally, that the decay of the EHD in lightly doped Ge at 2 °K should be determined by the lifetime of the EHD.

VI. SUMMARY AND CONCLUSIONS

We studied the time evolution of the EHD luminescence from pure and doped Ge using long surface-excitation pulses. We found the time required for droplet luminescence intensity to reach a steady state after excitation turn on to be several tens of microseconds in both pure and doped Ge. The long excitation pulses used in our experiment produced EHD decays in pure Ge which are much too slow to be explained by the independent-droplet model extensively used previously. In addition, it is shown that this independent-droplet model cannot account for the observed turn off of the net FE evaporation from EHD's in lightly doped Ge.

A new model for the EHD luminescence intensity decay which takes into account both the existence of a cloud of droplets and exciton emission and capture by droplets is presented. This model explains qualitatively the experiment results. In the case of pure Ge at 4.2 °K, evaporation from all the

droplets in the cloud keeps the exciton density inside the cloud at approximately the equilibrium density after the excitation is turned off. This exciton density implies that backflow is large within the cloud. This high exciton density causes the observed EHD decay times at 4.2 °K in pure Ge to be longer than expected from the independent droplet model. Pump-power dependence of the decay time is a consequence of the different initial cloud radii generated by different pump conditions.

For the lightly doped Ge the FE exciton diffusion length is reduced from that in pure Ge. This change in diffusion length can produce a large reduction in the rate of FE evaporation from the droplets. At sufficiently small diffusion lengths the droplets in our model act independently. The cloud does not shrink since excitons are not supplied to a substantial region outside the cloud or for that matter in between droplets. However, the evaporation of excitons from a given drop is nearly canceled by the recapture of those excitons by the same drop before they can diffuse away.

At 2 °K our model approaches an independent drop model. The FE density outside the EHD is quite small, evaporation is unimportant, and the primary decay mechanism is decay of pairs in the EHD. In this case the volume of a single drop decreases exponentially. These results are in agreement with the observed transients in the luminescence.

In summary, we measured the growth and decay of EHD luminescence in pure and lightly doped samples. We find that a model including the spatial variation of FE and EHD is in semiquantitative agreement with the observed decays.

ACKNOWLEDGMENTS

The authors are pleased to acknowledge R. N. Hall for supplying the high-purity Ge samples and K. R. Elliott for making his data available to us prior to publication. This work was supported in part by the Office of Naval Research under Contract No. N00014-75-C-0423. One of us (T.C.M.) would like to acknowledge the support of the Alfred P. Sloan Foundation.

APPENDIX

In this appendix the forms of $f(R_D)$ and $g(R_D, R_c)$ in Eq. (17) and (18) will be derived. First we will solve Eq. (7) for the interior of the cloud in order to obtain $\bar{n}_{ex}(t)$ and $N_0(t)$. As explained in Sec. III, we assume that each droplet has a volume associated with it and that there is no flow of excitons across the surface of this volume. We take this region to be a sphere of radius R_s defined by

$$R_s = [R_D^3(t=0)/F(t=0)]^{1/3}. \tag{A1}$$

The decay of a single drop is governed by

$$\frac{d}{dt}(n_0 V_D) = \frac{-n_0 V_D}{\tau} - J_D\big|_{R_D}, \tag{A2}$$

with n_0 the density of pairs in an EHD, V_D the average volume of a drop, and R_D the radius of the drop. Since n_0 is independent of time, we have

$$\frac{dR_D}{dt} = \frac{-R_D}{3\tau} - \frac{F_D|_{R_D}}{n_0}, \tag{A3}$$

where F_D is the flux of free excitons away from the surface. To find F_D we must solve the diffusion equation for the excitons with boundary conditions at R_D and R_s,

$$\frac{\partial n_{ex}}{\partial t} = D\nabla^2 n_{ex} - \frac{n_{ex}}{\tau_{ex}}. \tag{A4}$$

At $r = R_s$, $(\partial n_{ex}/\partial t) = 0$. At the surface of the drop, evaporation must balance backflow plus diffusion current away from the drop. In equilibrium, however, the backflow just balances the evaporation. So at $r = R_D$,

$$v_{th} n_{ex}^0(T) = v_{th} n_{ex}(r) + F_D, \tag{A5}$$

where v_{th} is the exciton thermal velocity and $n_{ex}^0(T)$ is the measured density of excitons in equilibrium with droplets as a function of temperature.

Defining $q = r n_{ex}$ and using the assumed spherical symmetry, the diffusion equation becomes

$$\frac{\partial q}{\partial t} = D\frac{\partial^2 q}{\partial r^2} - \frac{q}{\tau_{ex}}. \tag{A6}$$

Since we are in the interior of the cloud (and the fill factor is large enough for the cloud concept to be meaningful) q varies slowly with time, and we can make an adiabatic assumption that $\partial q/\partial t = 0$. This removes the explicit time dependence of $n_{ex}(r)$ though it still has an implicit time dependence through the boundary condition at R_D. The diffusion equation, Eq. (A6), has solutions of the form

$$n_{ex}(r) = \frac{q}{r} = \frac{R_D}{r} a_1 n_{ex}^0 [a_2 e^{-(r-R_D)/l_{ex}} + e^{(r-R_D)/l_{ex}}], \tag{A7}$$

where l_{ex} is the exciton diffusion length, $l_{ex} \equiv (D\tau_{ex})^{1/2}$, and a_1, a_2 are determined by the boundary conditions at R_D and R_s. If we let

$$\beta = v_{th} R_D / D, \tag{A8}$$

which is just the ratio of drop radius to exciton mean free path, and

$$\gamma = e^{(R_s - R_D)/l_{ex}}, \tag{A9}$$

then

$$a_2 = \gamma^2 [(R_s - l_{ex})/(R_s + l_{ex})], \tag{A10}$$

and

$$a_1 = [\beta/(\beta+1)(a_2+1)+(R_D/l_{ex})(a_2-1)]. \quad \text{(A11)}$$

This gives

$$\frac{F_D|_{R_D}}{n_0} = Da_1\frac{n_{ex}^0}{n_0}\left(\frac{a_2+1}{R_D}+\frac{a_2-1}{l_{ex}}\right). \quad \text{(A12)}$$

Substituting Eq. (A12) into Eq. (A3) we obtain

$$\frac{dR_D}{dt} = f(R_D), \quad \text{(A13a)}$$

with

$$f(R_D) \equiv -\frac{R_D}{3_\tau} + Da_1\frac{n_{ex}^0}{n_0}\left(\frac{a_2+1}{R_D}+\frac{a_2-1}{l_{ex}}\right), \quad \text{(A13b)}$$

which is Eq. (17) in the text. This equation is integrated numerically since a_1 and a_2 are complicated functions of R_D. From Eq. (A7) we obtain

$$\frac{\bar{n}_{ex}}{n_{ex}^0} \equiv \int_{R_D}^{R_s} 4\pi r^2 n_{ex}(r)\,dr/\tfrac{4}{3}\pi R_s^3 n_{ex}^0$$

$$= \frac{3a_1R_Dl_{ex}}{R_s^3}\left[(a_2-1)(R_0-l_{ex})+\frac{2a_2l_{ex}}{\gamma}\right], \quad \text{(A14)}$$

and

$$N_0 = n_0(R_D/R_s)^3. \quad \text{(A15)}$$

Now with $\bar{n}_{ex}$ and N_0 we can go back to the problem of the cloud as a whole. We need to determine the exciton diffusion profile outside the cloud to find $F_D|_{R_c}$, the flux of excitons at its surface. We have

$$\frac{\partial n_{ex}}{\partial_t} = D\nabla^2 n_{ex} - \frac{n_{ex}}{\tau_{ex}}, \quad [r>R_c(t)], \quad \text{(A16)}$$

and

$$\frac{\partial n_{ex}}{\partial t} = D\nabla^2 n_{ex} - \frac{n_{ex}}{\tau_{ex}} + \frac{3v_{th}F}{R_D}(n_{ex}^0 - n_{ex}), \quad [r \lesssim R_c(t)]. \quad \text{(A17)}$$

The first of these equations holds for excitons completely outside the region in which there are droplets ($r>R_c$). The second equation is for excitons just inside the edge of the cloud with the last term corresponding to the net evaporation of excitons per unit volume. This term leads to an average effective diffusion length for excitons within the cloud which is much smaller than l_{ex} and thus the perturbation in exciton concentration due to the cloud's surface extends in only a small distance.

In solving these equations, we must match the two solutions at $r=R_c(t)$ with boundary conditions $n_{ex}=0$ as $r\to\infty$ and $n_{ex}\to\bar{n}_{ex}$ as $r\to 0$. Deep inside the cloud $\bar{n}_{ex}$ satisfies the equation

$$\frac{\partial \bar{n}_{ex}}{\partial t} = \frac{-\bar{n}_{ex}}{\tau_{ex}} + \frac{3Fv_{th}}{R_D}(n_{ex}^0 - \bar{n}_{ex}). \quad \text{(A18)}$$

Defining $w \equiv \bar{n}_{ex} - n_{ex}$, and an effective lifetime due to capture by droplets $\tau_c \equiv R_D/3Fv_{th}$, then subtracting Eq. (A17) from Eq. (A18) yields

$$\frac{\partial w}{\partial t} = D\nabla^2 w - w\left(\frac{1}{\tau_{ex}}+\frac{1}{\tau_c}\right). \quad \text{(A19)}$$

For reasonable parameters (see Table I), $\tau_{ex}/\tau_c \sim 100$, and the effective diffusion length,

$$l_{eff} \equiv [D\tau_{ex}\tau_c/(\tau_{ex}+\tau_c)]^{1/2}, \quad \text{(A20)}$$

is given approximately by

$$l_{eff} \approx (D\tau_c)^{1/2}$$

and is quite short $l_{ex}/l_{eff} \approx 10$. Thus, the perturbation in exciton density due to the cloud's surface extends in only a short distance. Furthermore, τ_c is so short that the exciton profile within the cloud can react very rapidly to the motion of the surface as the cloud shrinks. This allows us to make an adiabatic approximation, setting $\partial w/\partial t = 0$ in the frame of reference of the cloud's surface and reducing the equation to steady state. Using spherical symmetry the resulting equation is readily solved, giving

$$w(r) = \frac{R_c}{r}w(R_c)\frac{(e^{r/l_{eff}} - e^{-r/l_{eff}})}{(e^{R_c/l_{eff}} - e^{-R_c/l_{eff}})}, \quad [r \lesssim R_c(t)], \quad \text{(A21)}$$

where the second term in the numerator keeps the solution finite at the origin and $w(R_c)$ must be determined by matching to the outside solution.

The solution to the equation for $r>R_c(t)$ is complicated by the fact that the exciton lifetime is too long to allow us to make the simple adiabatic assumption in this region we used in the $r \lesssim R_c$ case. Here the exciton profile does not simply move with the cloud's surface but it changes depending upon the velocity of the surface.

Assuming spherical symmetry and defining, $u \equiv [rn_{ex}/R_c(t)]$ and $v \equiv (-\partial R_c/\partial t)$, we can reduce the equation for $r>R_c$ to a one-dimensional form,

$$\frac{\partial u}{\partial t} = D\frac{\partial^2 u}{\partial_r{}^2} - u\left(\frac{1}{\tau_{ex}} - \frac{v}{R_c}\right). \quad \text{(A22)}$$

Now we transform to the frame stationary with respect to the cloud's surface by defining

$$x \equiv r - R_c(t). \quad \text{(A23)}$$

Defining $\tau' \equiv (R_c - \tau_{ex}v)/R_c\tau_{ex}$, the resulting equation is

$$\frac{\partial u}{\partial t} = D\frac{\partial^2 u}{\partial x^2} - v\frac{\partial u}{\partial x} - \frac{u}{\tau'}, \quad (x>0). \quad \text{(A24)}$$

Thus, to find $F_D|_{R_c}$, we must solve this equation subject to the boundary conditions that the inside and outside solutions match at R_c and that the den-

sity of excitons is zero at infinity:

$$\bar{n}_{ex} - w(R_c) = u(x=0), \tag{A25}$$

$$-\left.\frac{\partial w}{\partial r}\right|_{R_c} = \frac{\partial}{\partial x}\left(\frac{u}{R_c+x}\right)\Big|_{x=0}, \tag{A26}$$

and

$$u(\infty) = 0. \tag{A27}$$

The transformation has taken some of the time dependence out of u. The parts still left are

$$\frac{\partial n_{ex}(R_c)}{\partial t}, \quad \frac{\partial v}{\partial t}, \quad \frac{\partial \tau'}{\partial t}. \tag{A28}$$

If we assume that these terms are small, then we can make the adiabatic assumption and say $(\partial u/\partial t) = 0$. This assumption allows an analytic solution to Eq. (A24).

Defining

$$l' \equiv 2D/(v^2 + 4D/\tau')^{1/2} - v, \tag{A29}$$

the solution is

$$n_{ex}(r) = R_c(t) n_{ex}(R_c)[e^{(R_c - r)/l'}/r]. \tag{A30}$$

Matching the inside solution, Eq. (21), to the outside solution and using the fact that $R_c \gg l_{eff}$ gives

$$n_{ex}(R_c) = \bar{n}_{ex}[l'/(l' + l_{eff})](1 - l_{eff}/R_c). \tag{A31}$$

Balancing the density of carriers inside with the flux out gives

$$\frac{-dR_c}{dt} = \frac{D n_{ex}(R_c)}{N_0 + n_{ex}(R_c)}\left(\frac{1}{l'} + \frac{1}{R_c}\right), \tag{A32}$$

where $\partial l'/\partial t$ has been ignored since it is small when the adiabatic approximation is valid. Defining

$$\alpha \equiv 2[N_0 + n_{ex}(R_c)]/n_{ex}(R_c), \tag{A33}$$

we get the solution [ignoring the slight dependence on v of $n_{ex}(R_c)$]

$$\frac{dR_c}{dt} = g(R_D, R_c), \tag{A34a}$$

with

$$g(R_D, R_c) \equiv \frac{-4D}{R_c(\alpha+1)} - \frac{\{(\alpha-1)[\alpha+1-2(l_x/R_c)^2]\}^{1/2}}{\alpha^2 - 1}. \tag{A34b}$$

This is the equation given in the text as Eq. (18). N_0 and $\bar{n}_{ex}$ are functions of R_D and thus α is a function of $R_D(t)$.

Thus, we have reduced the problem to two consecutive numerical integrations. First Eqs. (A13a) and (A13b) are integrated to obtain $R_D(t)$, and from it $\bar{n}_{ex}(t)$ [Eq. (A14)] and $N_0(t)$ [Eq. (A15)] may be found. These functions are then used in the integration of Eqs. (A34a) and (A34b) to find $R_c(t)$. It is most convenient to calculate the exciton luminescence by breaking it up into the contribution from excitons within the cloud and the contribution from those outside [Eq. (20a)]. The source-sink equation [Eq. (20b)] is used to find the term arising from excitons outside the cloud. This avoids the problem of a careful calculation of the exciton profile which would be needed for a spatial integration to determine I_{FE}. The effective diffusion length l' is a good characterization of the diffusion profile near the cloud's surface since it arises from the surface moving past some excitons and thus giving less slope to the profile than just l_{ex}. However, far from the cloud edge the exciton profile is not a simple exponential due to the acceleration of the surface of the cloud.

The theoretical curves were calculated with initial conditions chosen so as to avoid transients at the beginning. Thus, it was assumed that the cloud and droplet edges have a finite velocity at $t = 0$. This was found by determining the diffusion profiles within the cloud to get $\bar{n}_{ex}$, and then solving self-consistently for $\partial R_c/\partial t$. The self-consistent approach is necessary to correctly include the dependence of $n_{ex}(R_c)$ on v. The number of excitons outside the cloud at the beginning of the calculation $M_{ex}(0)$ is determined by spatially integrating the solutions for $n_{ex}(r)$ at $t = 0$.

[1] C. D. Jeffries, Science 189, 955 (1975), and references contained therein.

[2] J. C. V. Mattos, K. L. Shaklee, M. Voos, T. C. Damen, and J. M. Worlock, Phys. Rev. B 13, 5603 (1976), and references contained contained therein.

[3] K. L. Shaklee, in *Proceedings of Third International Conference on Light Scattering in Solids, Campinas, Brazil, 1975*, edited by M. Balkanshi, R. C. C. Lute, and S. P. S. Porto (Flammarion, Paris, 1976), p. 160.

[4] J. M. Hvam and O. Christenson, Solid State Commun. 15, 929 (1974).

[5] V. S. Bagaev, N. A. Penin, N. N. Sibel'din, and V. A. Tsvetkov, Fiz. Tverd. Tela. 15, 3269 (1973) [Sov. Phys.-Solid State 15, 2179 (1974)].

[6] J. C. Hensel, T. G. Phillips, and T. M. Rice, Phys. Rev. Lett. 30, 227 (1973).

[7] C. Benoit à la Guillaume, M. Capizzi, B. Etienne, and M. Voos, Solid State Commun. 15, 1031 (1974).

[8] R. M. Westervelt, T. K. Lo, J. L. Staehli, and C. D. Jeffries, Phys. Rev. Lett. 32, 1051 (1974).

[9] B. M. Ashkinadze and I. M. Fishman, Fiz. Tekh. Poluprovodn. 11, 408 (1977) [Sov. Phys.-Semicond. 11, 235 (1977)].

[10] K. Fujii and E. Otsuka, Solid State Commun. 14, 763 (1974).

[11] J. Shah, A. H. Dayem, M. Voos, and R. N. Silver,

Solid State Commun. 19, 603 (1976).
[12]J. L. Staehli, Phys. Status Solidi B 75, 451 (1976).
[13]R. N. Silver, Phys. Rev. B 11, 1569 (1975); B 12, 5689 (1975).
[14]R. M. Westervelt, Phys. Status Solidi B 74, 727 (1976); B 76, 31 (1976).
[15]Y. E. Pokrovskii, Phys. Status Solidi, A 11, 385 (1972).
[16]To apply to the excitons, the Richardson-Dushman constant for metals is corrected for exciton mass, binding energy, and degeneracy. In addition, a factor $(36)^{1/3}n_0^{2/3}$ is incorporated in which converts in $n^{2/3}$ to the droplet surface area.
[17]C. Benoît à la Guillaume and M. Voos, Solid State Commun. 11, 1585 (1972).
[18]D. L. Smith, Solid State Commun. 18, 637 (1976).
[19]M. Chen, D. L. Smith, and T. C. McGill, Phys. Rev. B 15, 4983 (1977).
[20]J. Doehler, J. C. V. Mattos, and J. M. Worlock, Phys. Rev. Lett. 38, 726 (1977).
[21]K. R. Elliott, D. L. Smith, and T. C. McGill (unpublished).
[22]R. W. Martin, Phys. Status Solidi B 61, 223 (1974).
[23]M. Chen (unpublished).